Theory of Simple and Complex Materials

Sergei I. Simak

Linköping University (Sweden)

NSC'09 , *Linköping, October 13-14 (2009)*

Simple and Complex structures

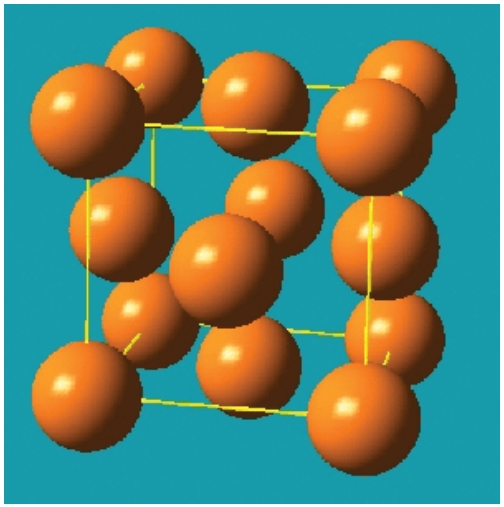

Au

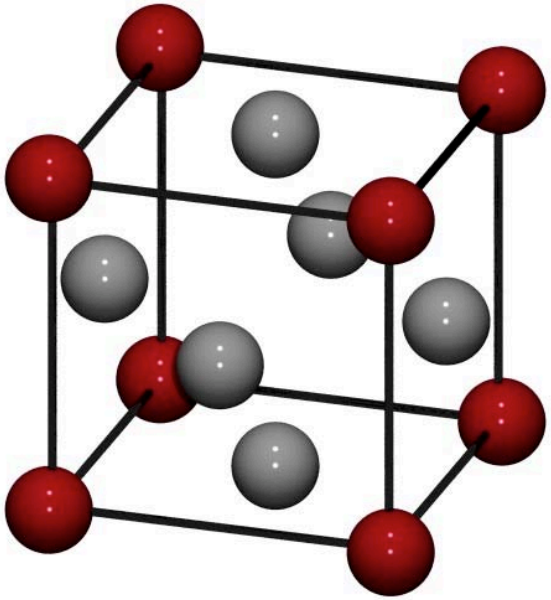

Cu_3Au

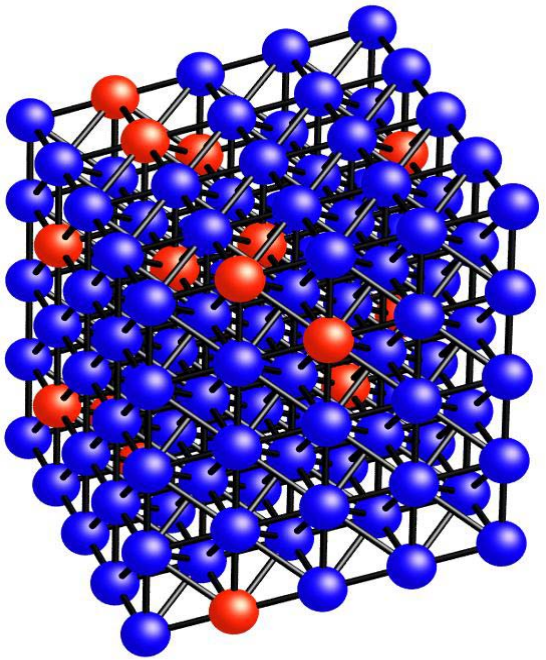

Fe-Ni alloy

First-principles calculations of materials at given external conditions (pressure, temperature etc.)

- Quantum mehanics
- Density Functional Theory (DFT) within LDA, GGA, …
- All-electron or pseudopotential methods
  - PAW
  - FP-LMTO
  - Ultrasoft or norm-conserving pseudopotential techniques
  - …
- Total energy vs. volume calculations (T = 0 K)
- Phonon spectra (T ≠ 0 K, harmonic approximation)
- Molecular dynamics (T ≠ 0 K, anharmonicity is taken into account)
- …

What kind of information can be extracted?

What is the accuracy provided by first-principles methods?

…

Calculations and problems:

- Matrix diagonalization
- Fourier transformations
- Poisson equation
- Integration over the Brillouin zone (k-points)
- …

- Scaling with the number of atoms, N, is at worst as N^3
- Scaling with respect to the number of k-points is basically linear
- Massive parallelization
- Scaling
- Optimization
- Stability

Gold under high pressure

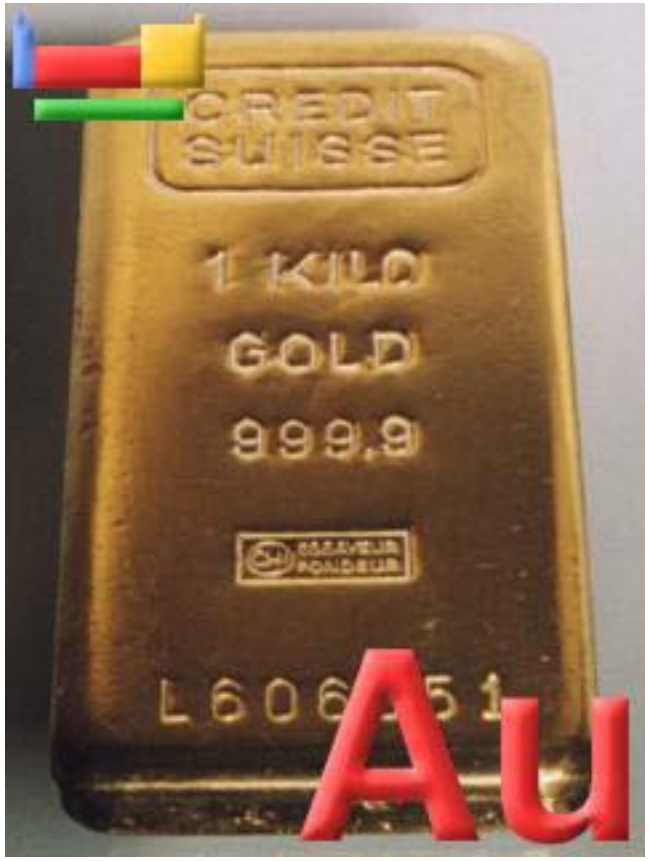

Why gold?

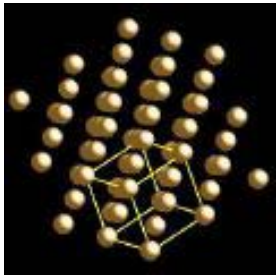

Stability of the solid phase of gold in its face-centered cubic (fcc) structure at pressures up to at least 180 GPa has been shown experimentally.

Gold has been in focus of high pressure research for several decades as a primary equation of state (EOS) standard.

Advances in high-pressure techniques require standards which are applicable at multimegabar pressure range. Large pressure and temperature stability ranges of the fcc phase and its large isothermal compressibility make gold a very attractive material to be used as a pressure marker above 100 GPa.

Possible pressure-induced phase transition in gold will place a ‘‘natural’’ limit on the application of fcc-Au as a standard.

Examples of gold diffraction patterns (DAC experiments)

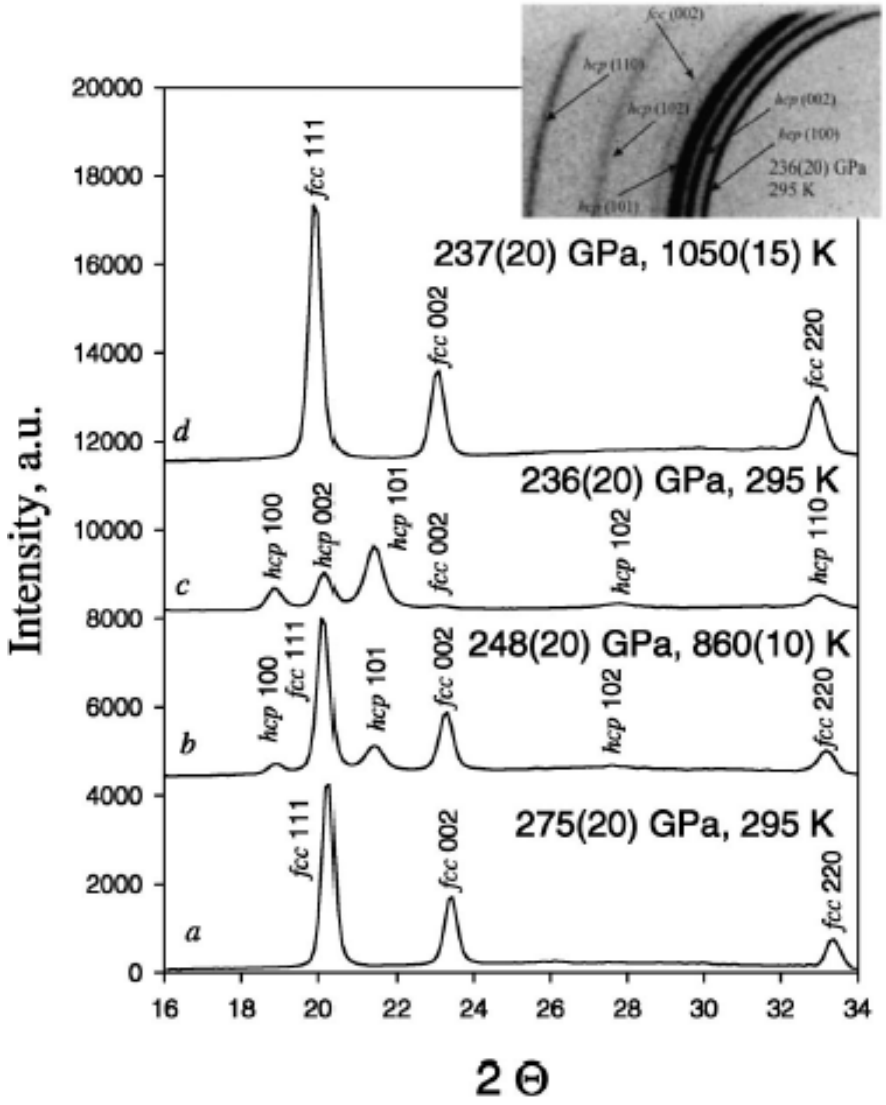

The inset shows part of 2D diffraction image of the sample at 236(20) GPa and room temperature. The pattern is dominated by diffraction lines of the high-pressure hcp-Au phase.

(d) heated again to 1050(15) K at 237(20) GPa

(c) slowly cooled down to room temperature at 236(20) GPa

(b) heated at 860(10) K at 248(20) GPa

(a) compressed at ambient temperature to 275(20) GPa,

Phys. Rev. Lett. **98,** 045503 (2007)

Pressure dependencies of the Gibbs free energy of the *hcp* and *dhcp* phases of Au

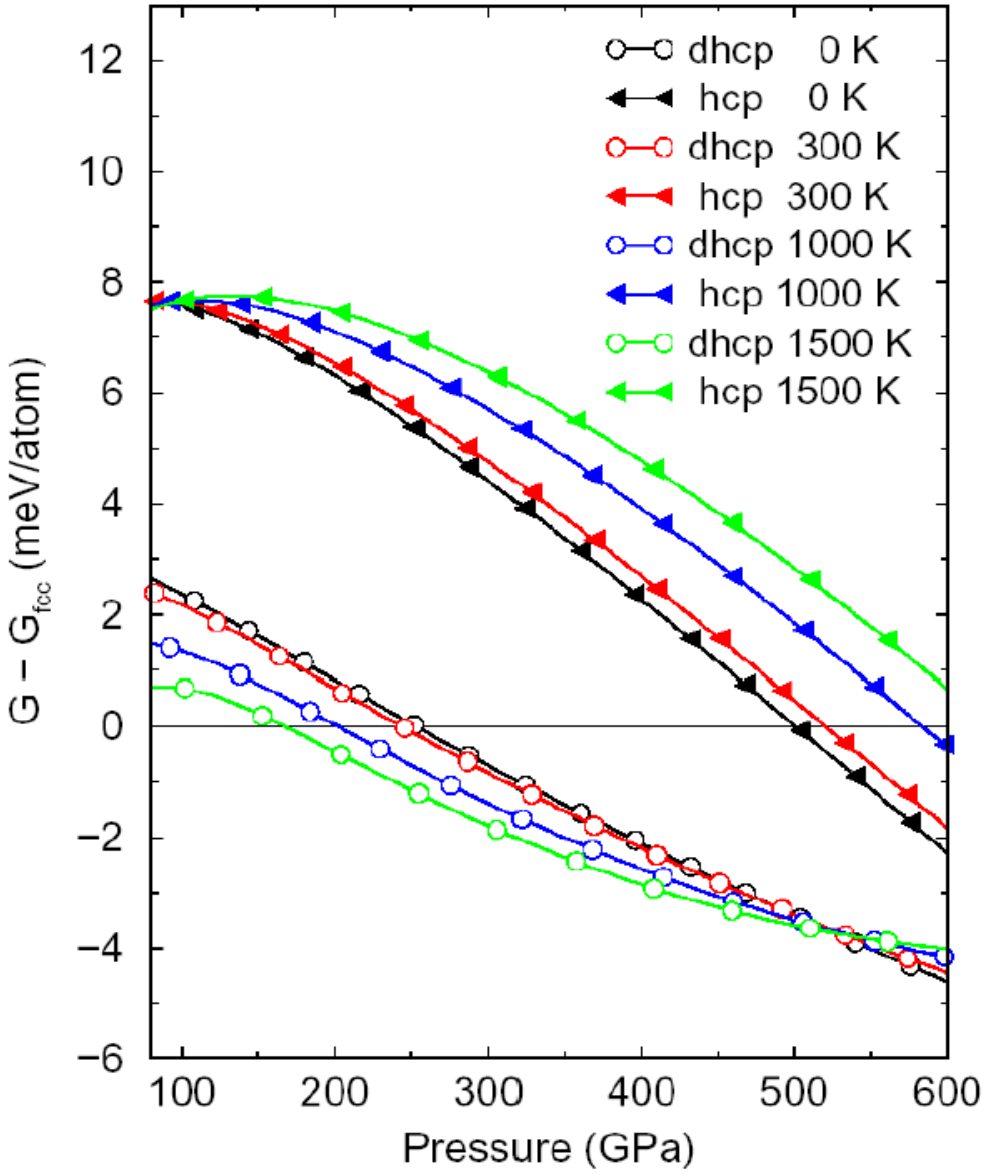

All the energies are presented relative to the Gibbs free energy of the *fcc* phase at temperatures equal to 0, 300, 1000, and 1500 K, respectively.

Close-packing

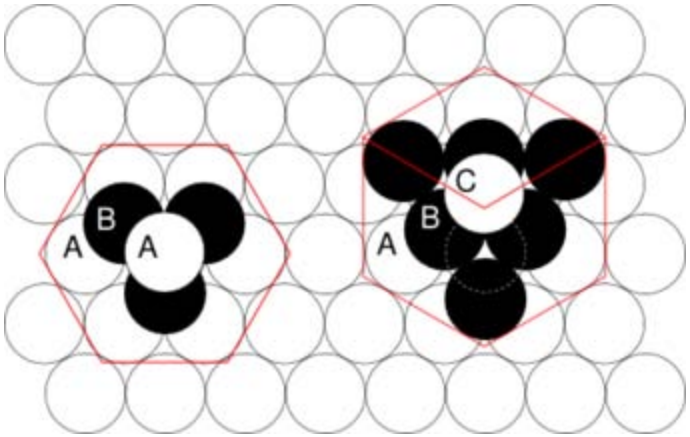

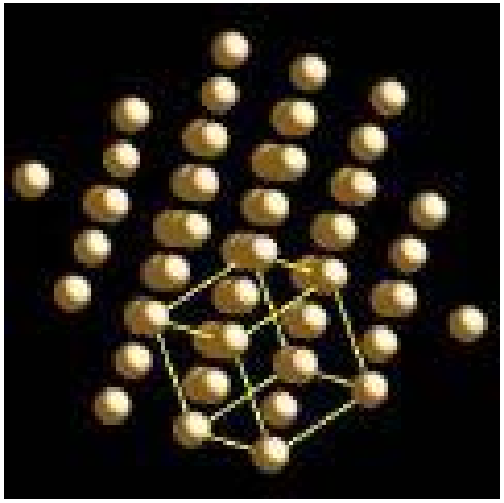

ABABAB… ABCABC…

HCP FCC

Calculated enthalpies of different arrangements of the close-packed atomic layers in gold under compression.

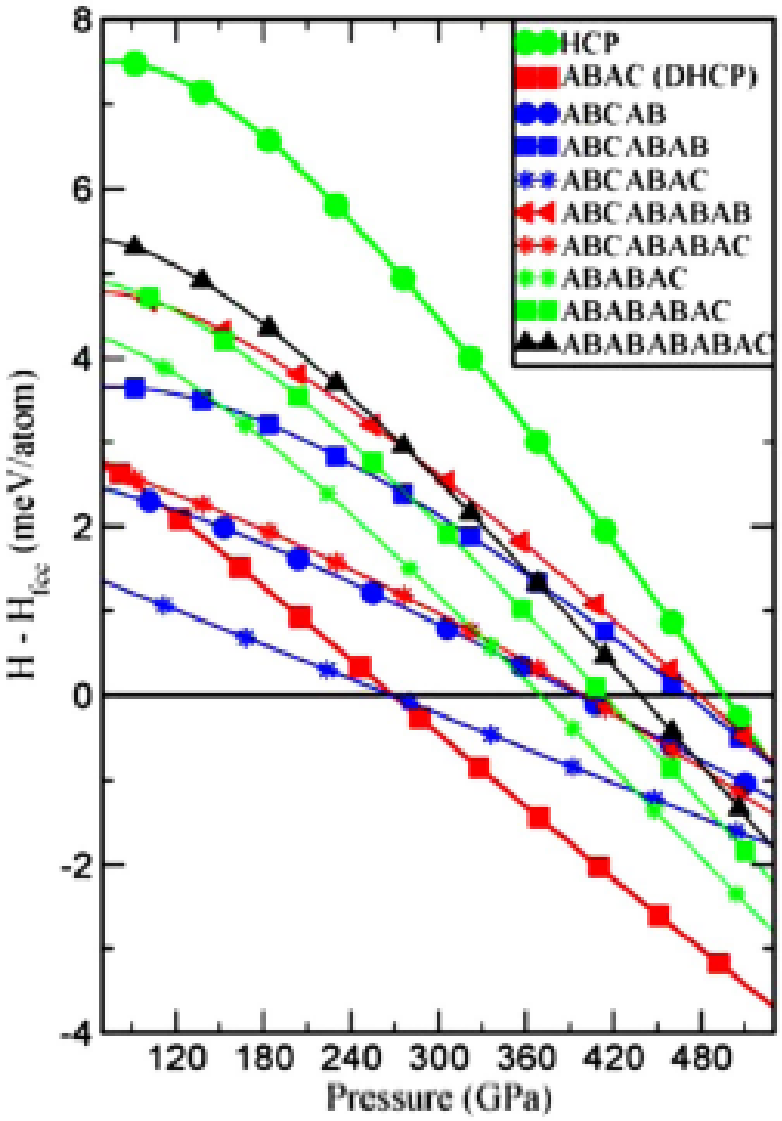

Enthalpies are given with respect to the enthalpy of the fcc phase.

Phys. Rev. Lett. **98,** 045503 (2007)

Iron in the Earth's core

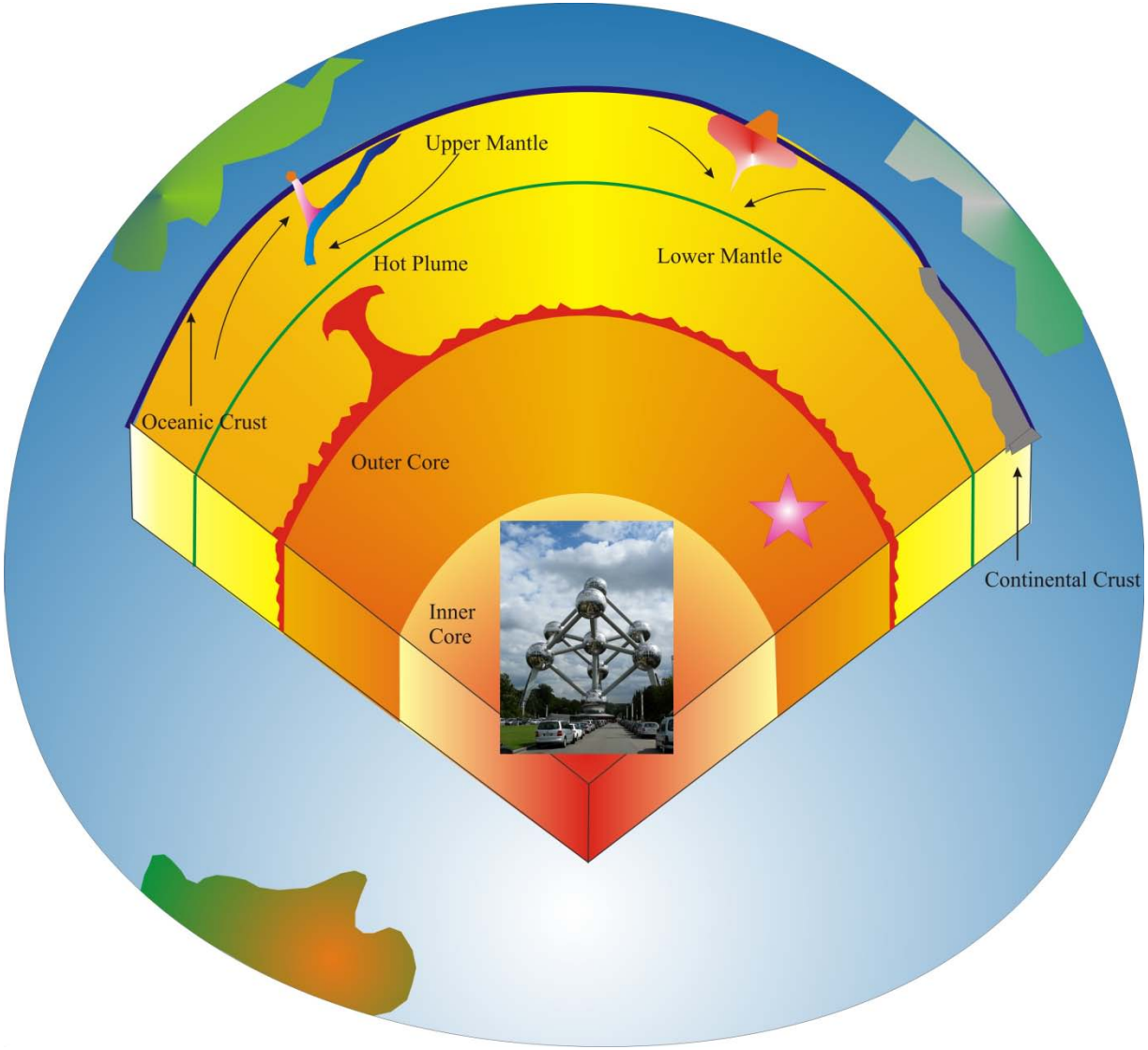

Pure Iron Compressed and Heated to Extreme Conditions

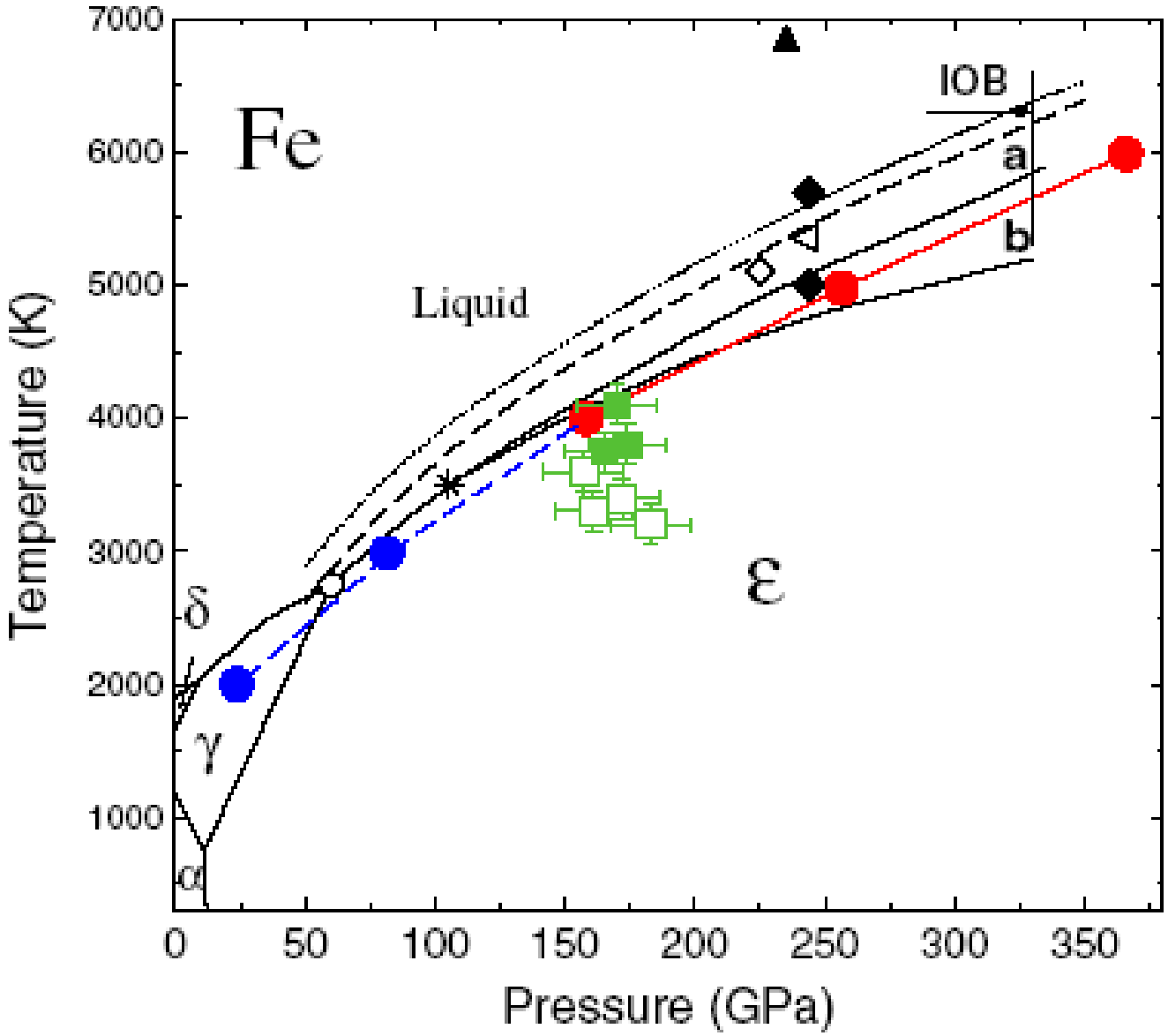

Motivation

Results of shock-wave experiments by Brown and McQeen indicate a post-hcp solid-solid phase transition at P = 200-240 GPa and T = 5000-5500 K.

Above the triple point fcc – hcp – liquid the fcc phase has never been observed. The slope of the hcp – fcc phase transition line, extrapolated to the very high pressure seems to rule out a possibility of the re-appearance of the fcc phase of Fe up to the Earth's core conditions.

According to previous theoretical estimations the fcc structure is less stable than both the hcp and dhcp structures at high pressure and temperature.

Calculated Gibbs energy difference between the fcc and the hcp phases of Fe as a function of pressure at different temperatures.

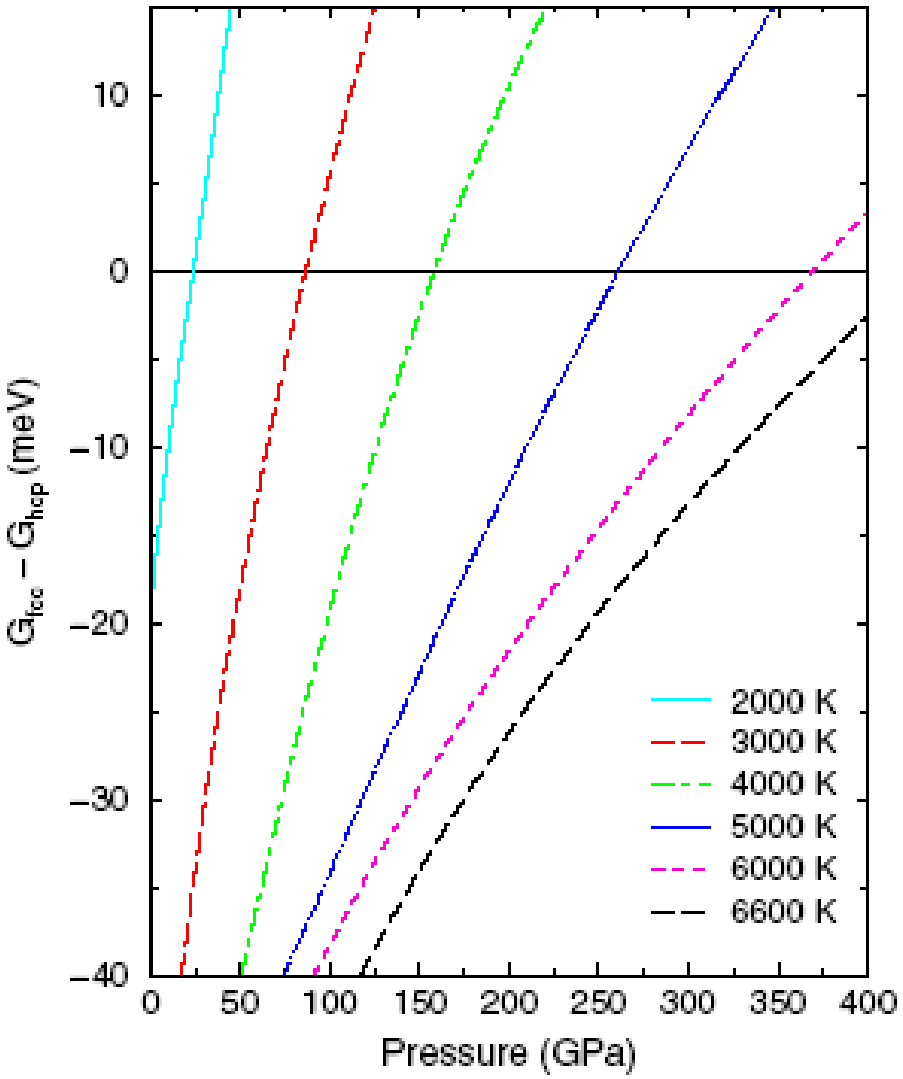

Pure Iron Compressed and Heated to Extreme Conditions

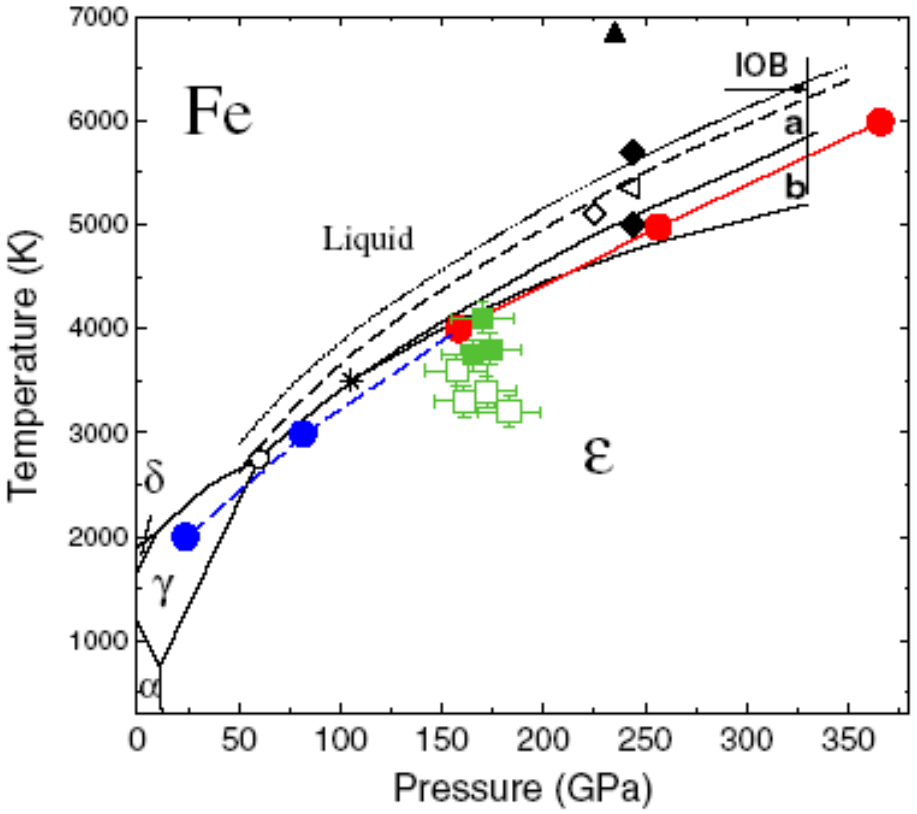

ε-γ-liquid triple point

(a) melting curve from the Lindeman's law

(b) melting curve from Kraut-Kennedy law,

melting points from the shock-wave data

melting point from Yoo *et al.*

--- and .-.-.- theoretical estimation of the melting temperature from molecular-dynamics study with and without free energy correction, respectively, from Alfe *et al.*.

IOB = inner-core–outer-core boundary

and ● fcc-hcp phase boundary obtained theoretically

and ■ correspond to the present experimental points for homogeneous hcp-Fe phase and the fcc-hcp phase mixture, respectively.

Phys. Rev. Lett. **99,** 165505 (2007)

Dubrovinsky et al., Science June 2007

Body-Centered Cubic Iron-Nickel Alloy in Earth's Core

L. Dubrovinsky,[1] N. Dubrovinskaia,[2] O. Narygina,[1] I. Kantor,[1] A. Kuznetzov,[3] V. B. Prakapenka,[3] L. Vitos,[4,5,6] B. Johansson,[4,5] A. S. Mikhaylushkin,[6,7] S. I. Simak,[7] I. A. Abrikosov[7]

Cosmochemical, geo… Earth's core contains iron with substantia… $_9Ni_{0.1}$ has been studied in situ by m… ted diamond anvil cells (DACs), and its… and temperature. At pressures above 22… $_{0.1}$ adopts a body-centered cubic struc… pport the interpretation of sh… transition above about 200 gigapasc… easonable compositions (that i… the bcc structure in Earth's inner core.

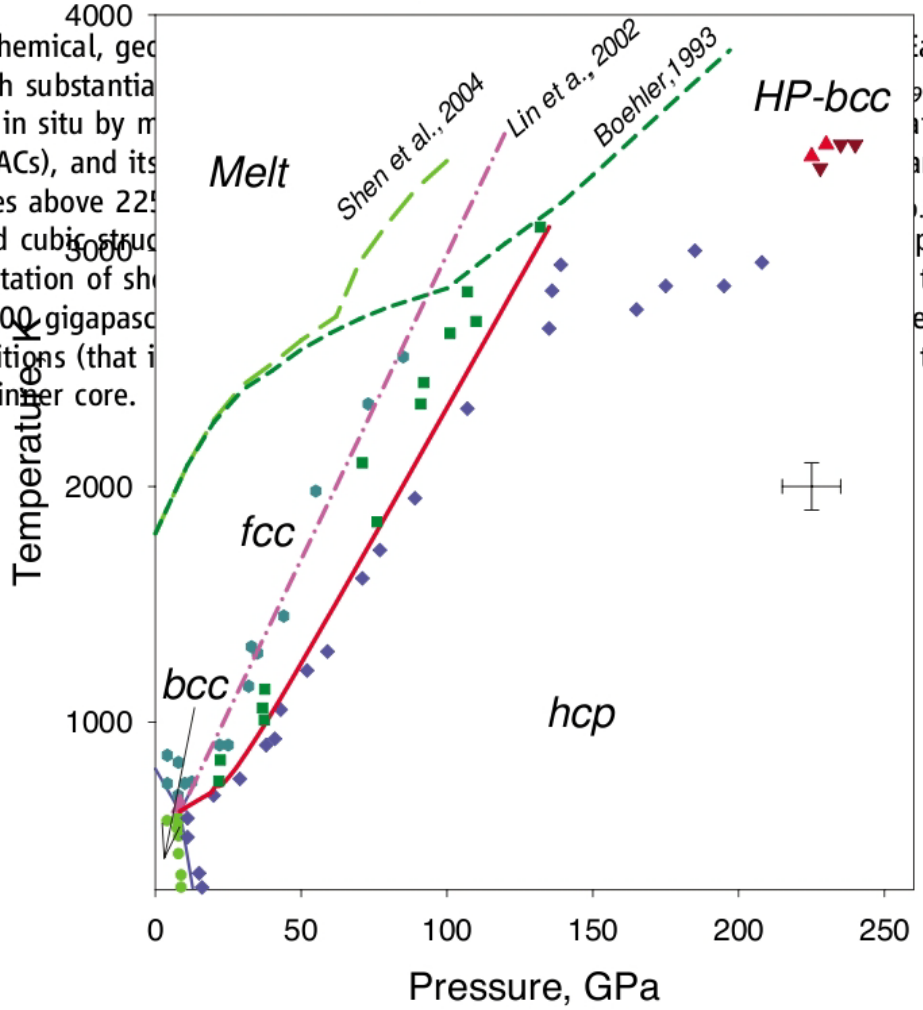

Fe at high pressures at T = 0 K

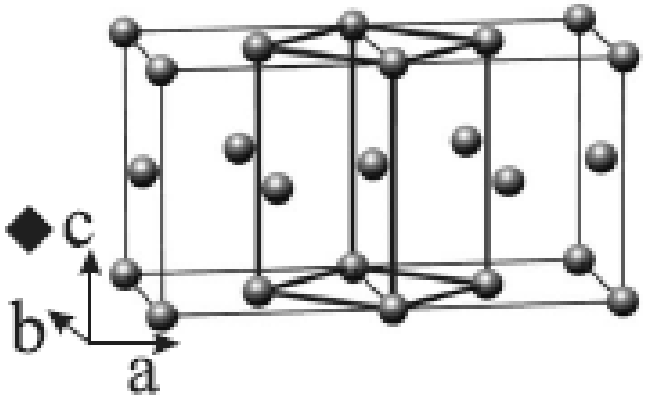

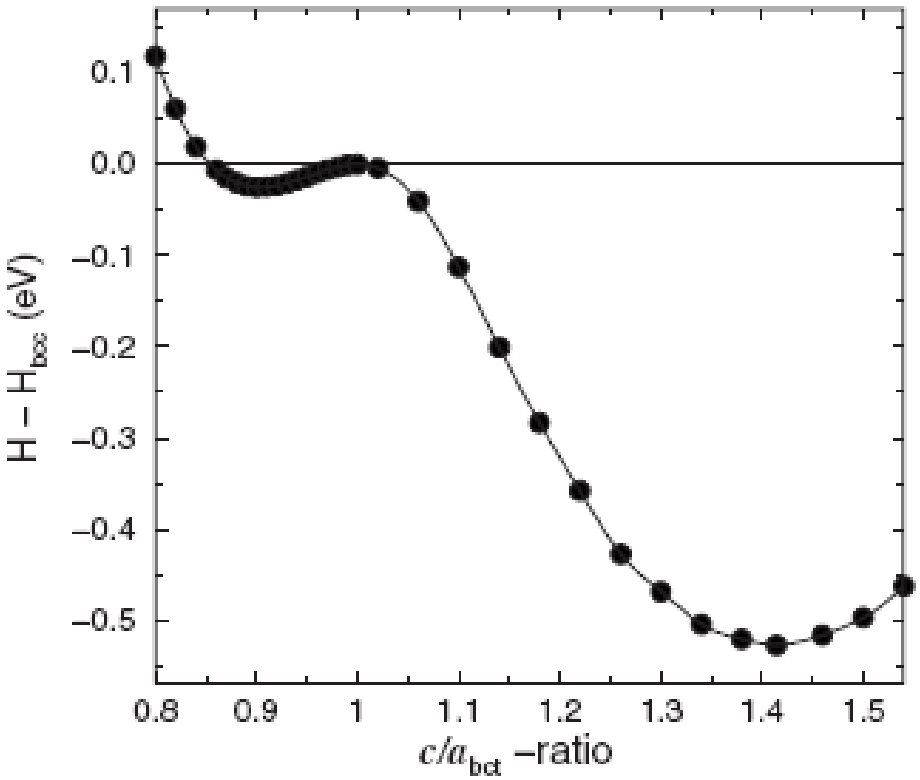

P ~ 330 GPa T = 0 K

bcc Fe+12.5% Ni: a molecular dynamics study

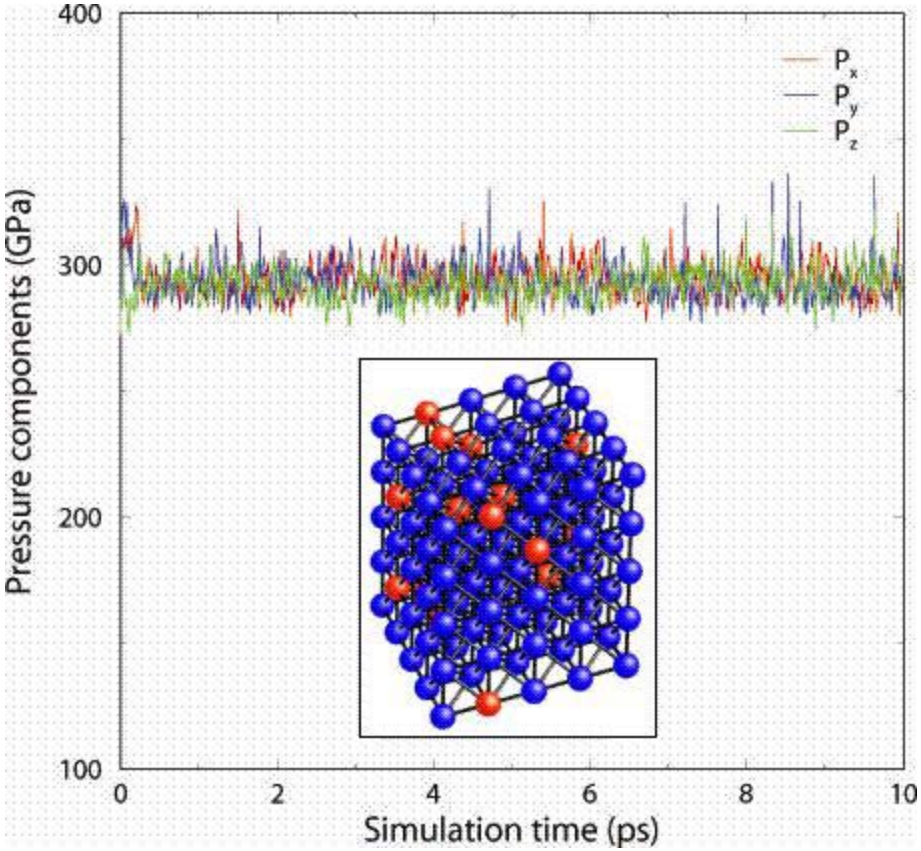

Results of *ab-initio* molecular dynamics simulations of Fe-rich FeNi alloy with the bcc crystal structure at 300 GPa and 6000 K. Shown are diagonal stress components as a function of simulation time. There is no deviation between the average values of the pressure components for *x, y,* and *z*-directions. This indicates the dynamical stability of the bcc structure of the alloy, represented by the large supercell with quasi-random distribution of Fe (blue) and Ni (red) atoms (see inset).

Fuel cells as the future power source?

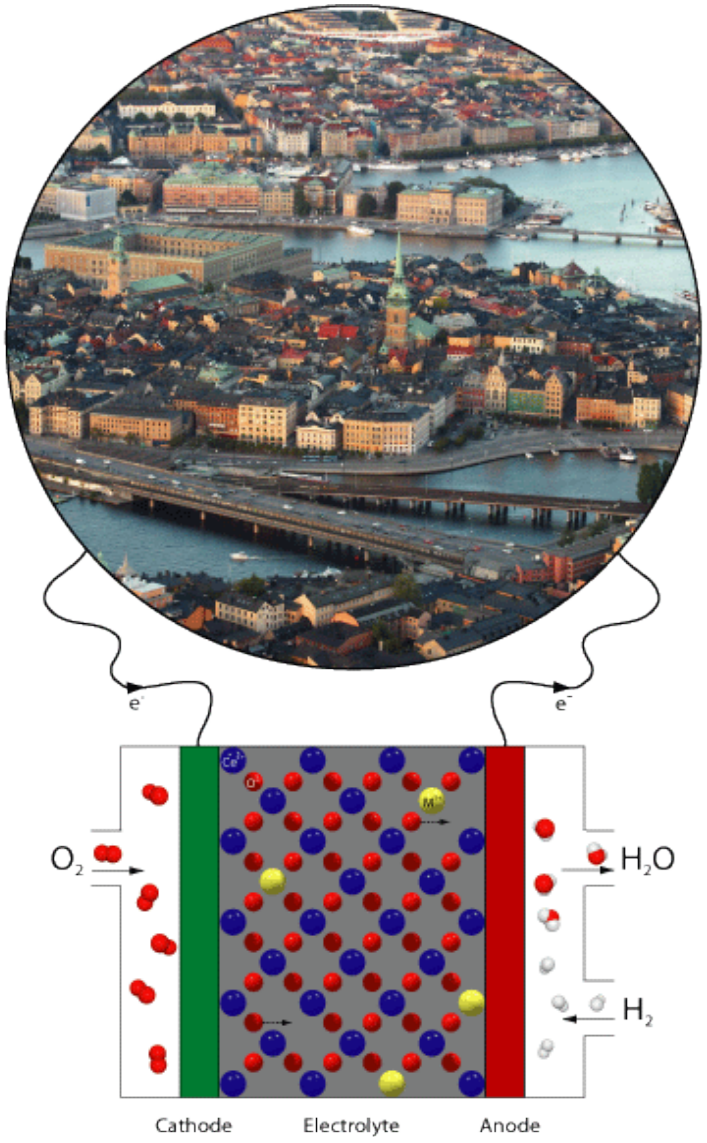

Solid oxide fuel cell, including ceria electrolyte

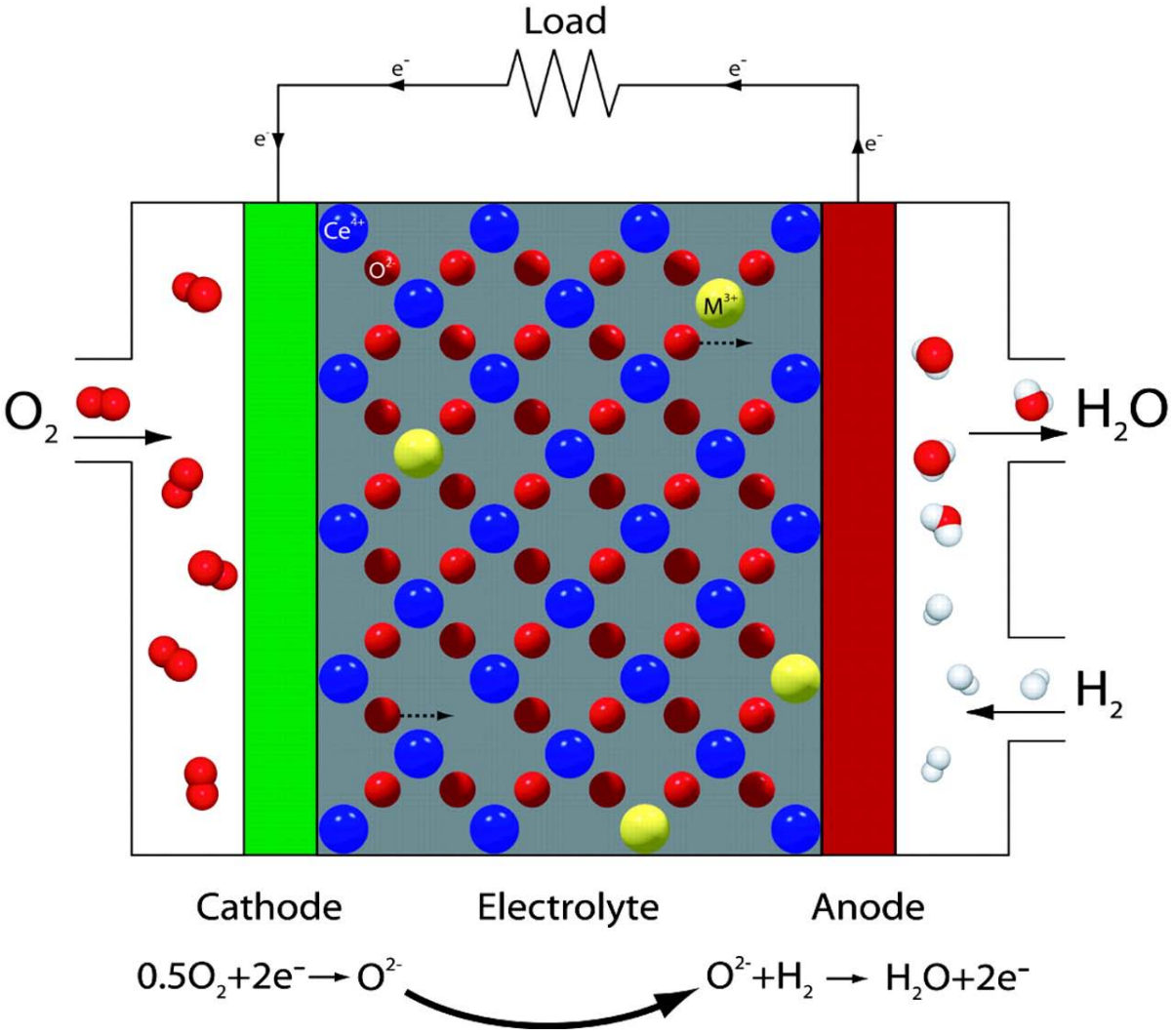

Oxygen storage in modern cars: the role of ceria

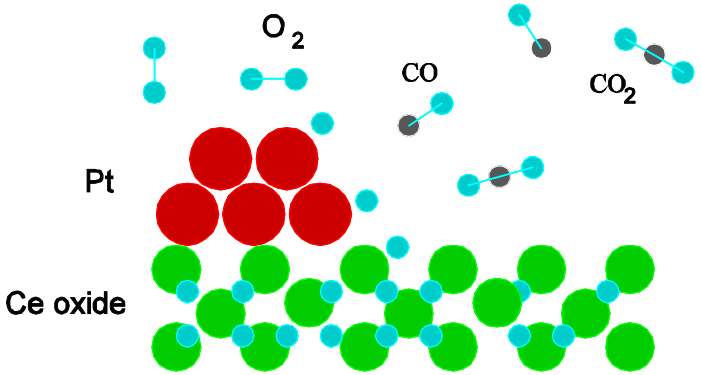

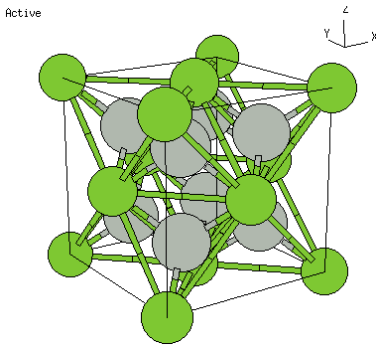

$$Ce\,O_2 \longleftrightarrow Ce_2\,O_3$$

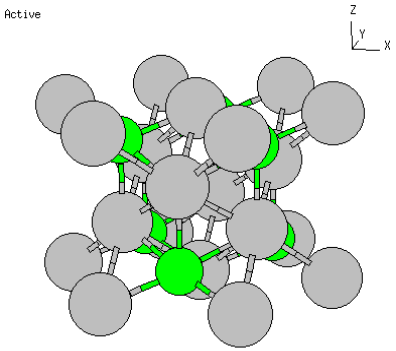

delocalized 4f electron of Ce

localized 4f electron of Ce

Ground-State Crystal Structures of CeO_2 and Ce_2O_3

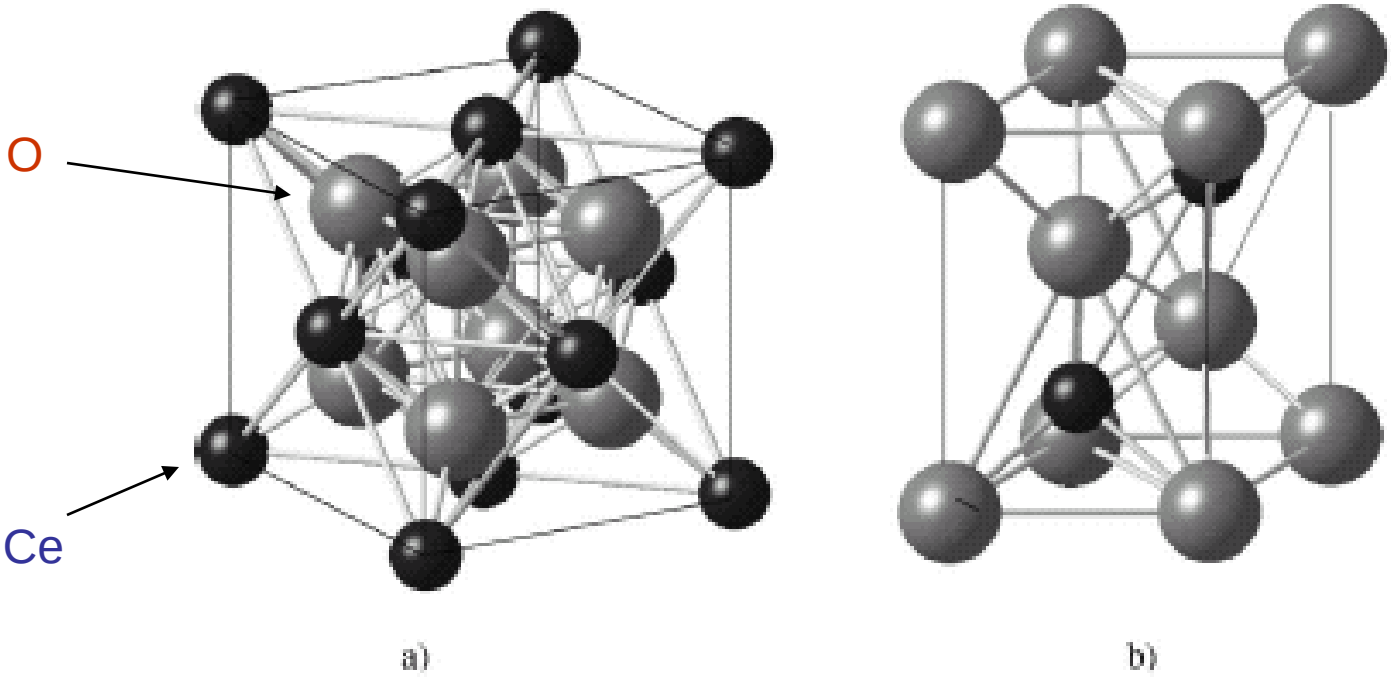

a) Cubic fluorite lattice of CeO_2
b) Hexagonal lattice of Ce_2O_3.
Ce and O atoms are shown by black and gray circles, respectively.

Energetics of vacancy formation in CeO_2

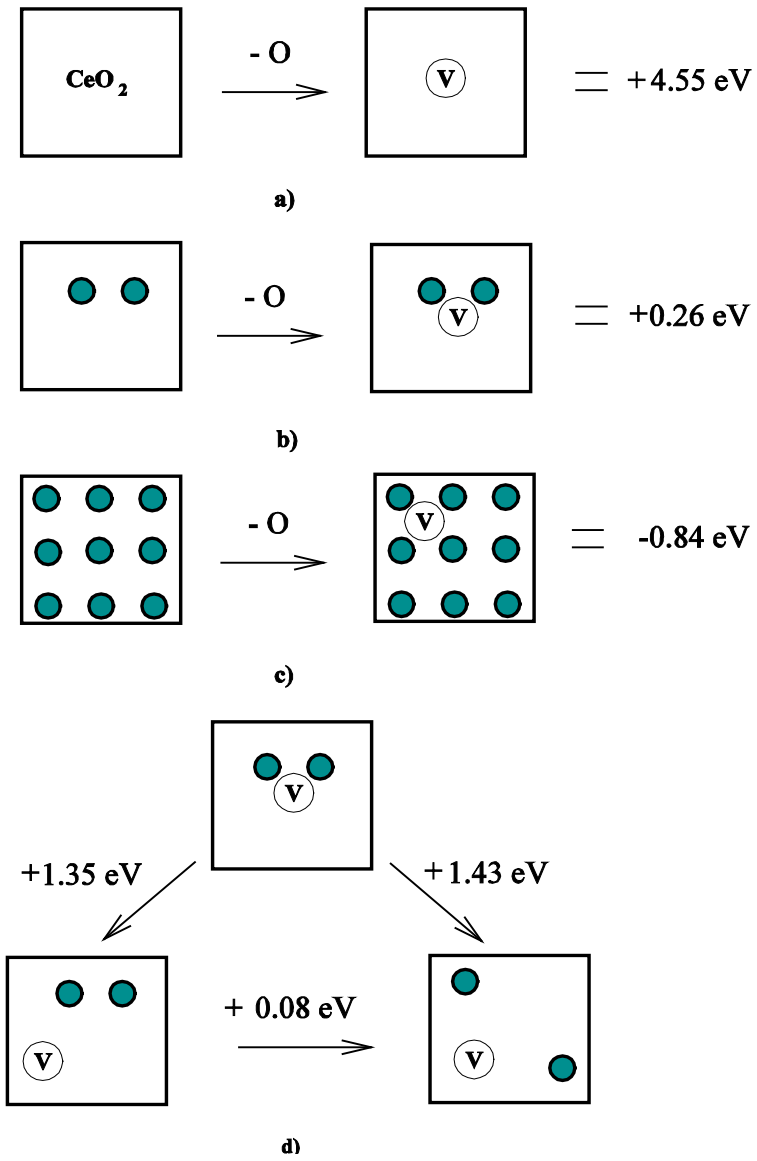

a) Vacancy formation in the perfect CeO_2 crystal requires 4.55 eV. The 4f electrons of all Ce atoms are treated as valence electrons.

b) Vacancy formation next to a pair of Ce(3+) atoms embedded into the CeO_2 crystal requires only 0.26 eV. The Ce(3+) the 4f-electrons are treated as firmly localized, i.e. core electrons.

c) Vacancy formation in the crystal of CeO_2 structure containing only Ce(3+). The removal of an oxygen atom gives an energy gain of 0.84 eV.

d) The most favorable position of Ce(3+) atoms in the CeO_2 matrix is next to an oxygen vacancy.

Phys. Rev. Lett. 89, 166601 (2002)

Quantum origin of the oxygen storage capability of ceria

The microscopic mechanism behind the extraordinary ability of ceria to store, release, and transport oxygen can be understood on the basis of first-principles quantum-mechanical simulations.

The reversible CeO_2 - Ce_2O_3 reduction transition associated with oxygen vacancy formation and migration appears to be directly coupled with the quantum process of electron localization.

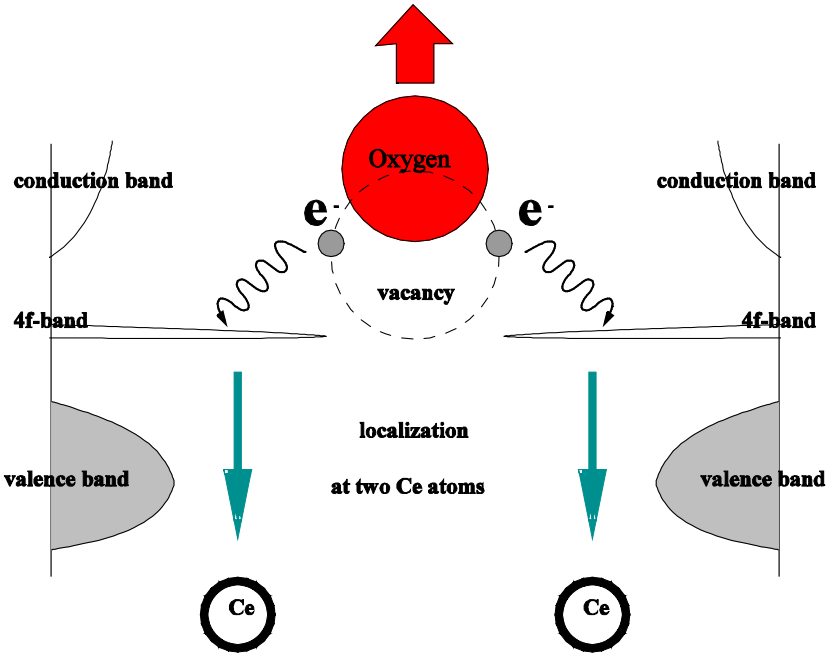

The schematic process of oxygen vacancy formation in ceria.

Phys. Rev. Lett. 89, 166601 (2002)

Reduction T: $Ce_{1-y}M_yO_2 \leftrightarrow Ce_{1-y}M_yO_{1.9688}+0.0156O_2$, M=Ce, Ti, Zr, Hf or Th, as function of P_{O2}

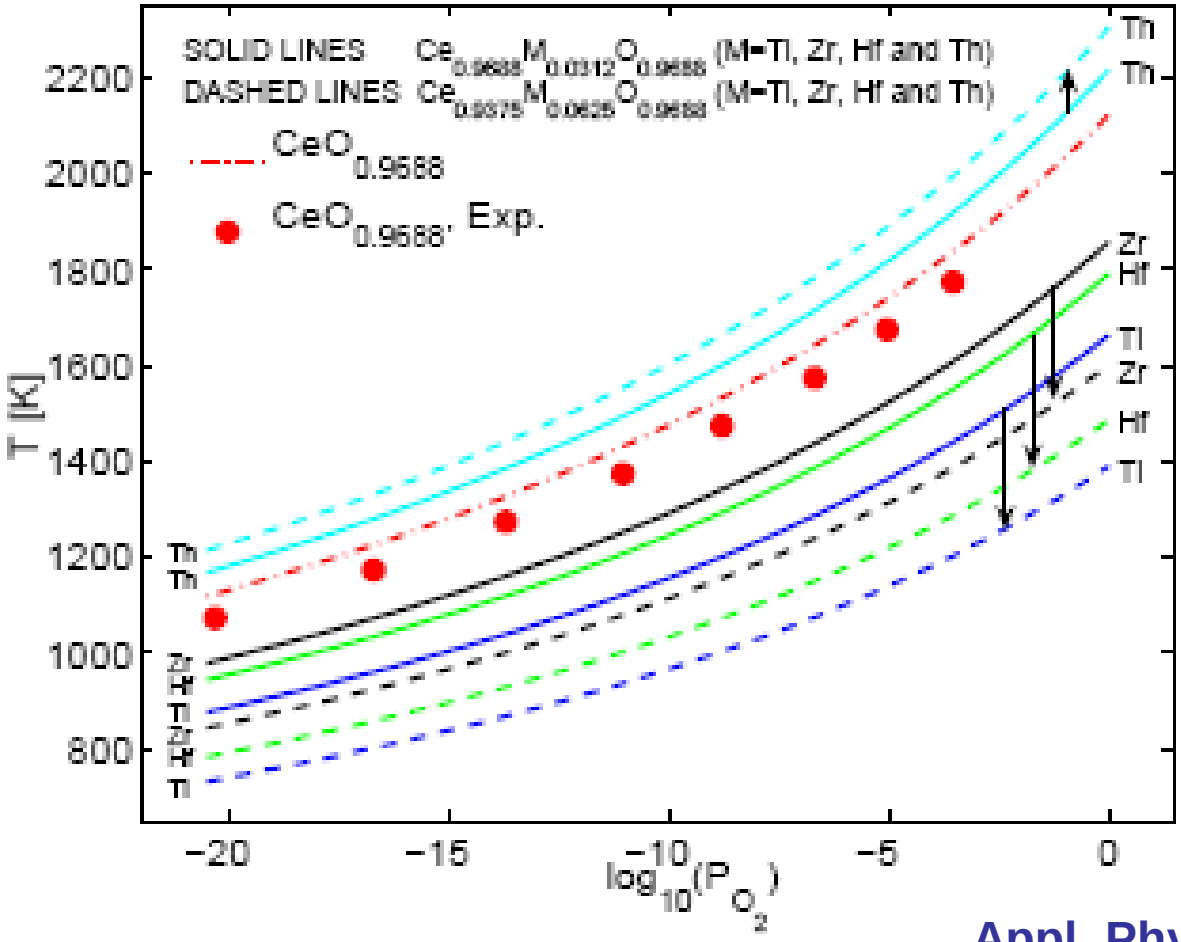

- Reduction: T decreases significantly for Ti, Zr and Hf
- Good for oxygen storage capacity
- Ti gives the largest improvement
- Th increases reduction T

Appl. Phys. Lett. 90, 031909 (2007)

Solid oxide fuel cell, including ceria electrolyte

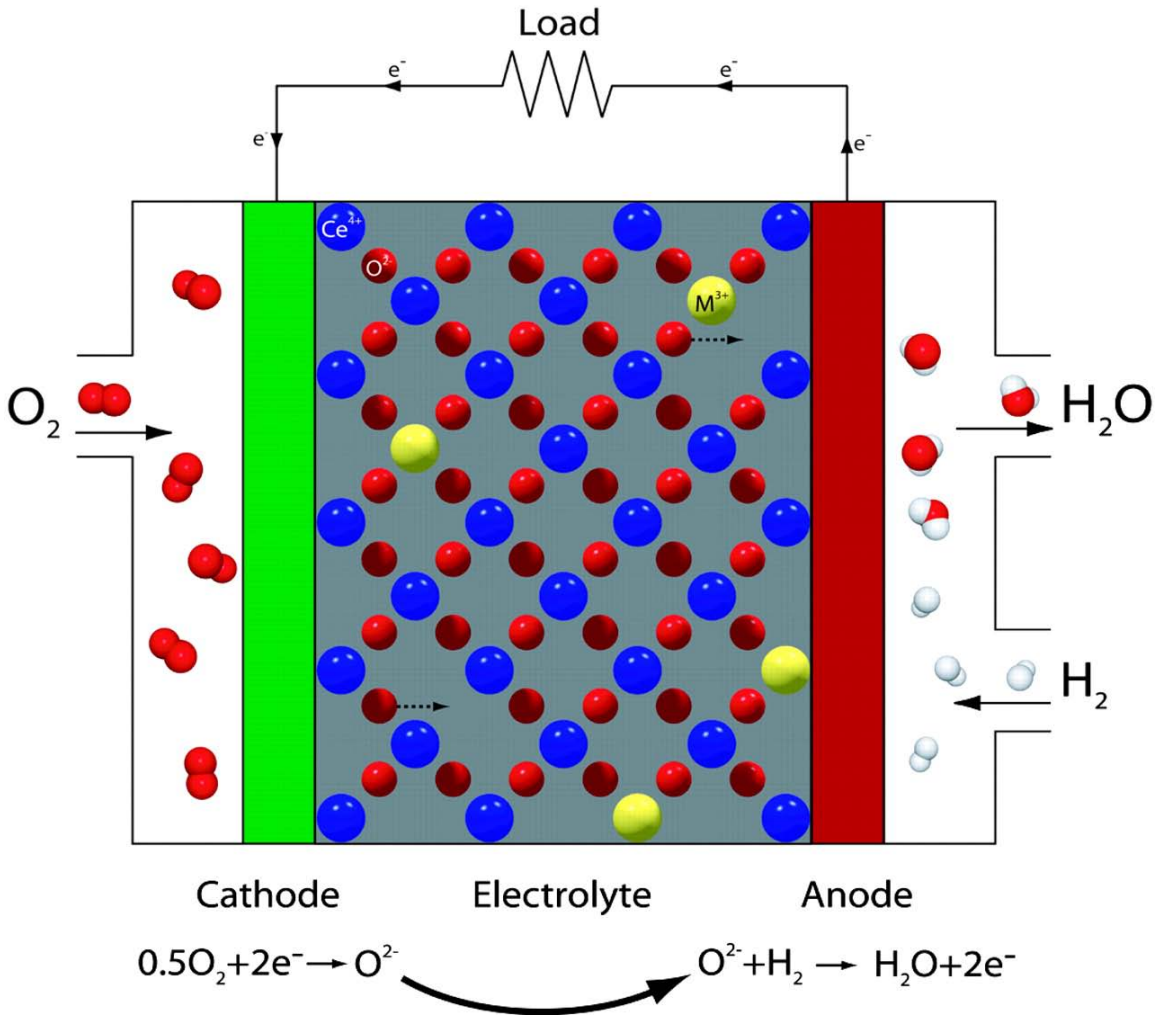

- Ionic conductivity: $\sigma \sim \exp(-E_a/k_BT)$, where E_a stands for the activation energy for oxygen vacancy diffusion, T for temperature.
- Currently: SOFC's operating temperatures ~1000°C
- How to decrease the SOFC's operating temperatures is an important question for fuel cell development.

Oxygen vacancy diffusion parameters in doped ceria

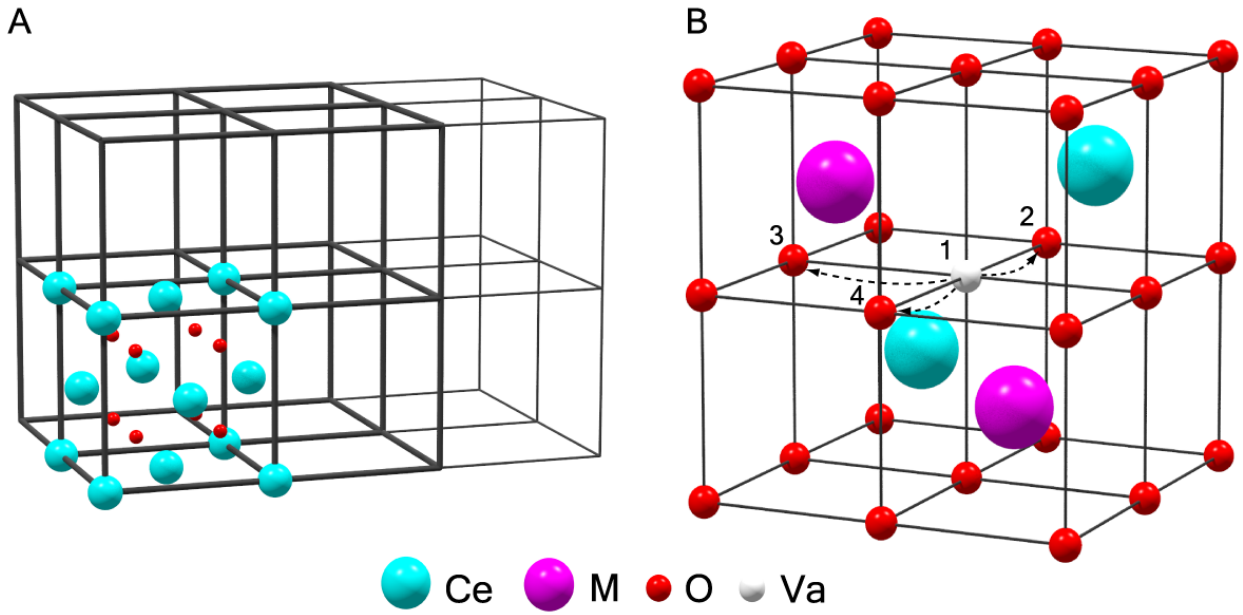

(A)The 2x2x2 (96 sites) supercell of ceria (thick lines) and the 3x2x2 (144 sites) supercell (thick and thin lines). Atoms are shown in one of the ceria unit cells. (B) A unit cell of ceria centered at the cubic oxygen sublattice. The cell contains two 3+ dopants (M) sitting next to each other and an oxygen vacancy. The numbers designate different locations that the vacancy can occupy with respect to the dopants, and the arrows schematically show how the vacancy can jump from site 1 to nearby sites, which is equivalent to oxygen diffusion in the opposite direction. Site 1 corresponds to the NN position and site 2 to the NNN position. A vacancy moving from site 1 to site 2 is labeled as 1_2. Other diffusion paths are labeled correspondingly.

Calculated defect formation and migration parameters

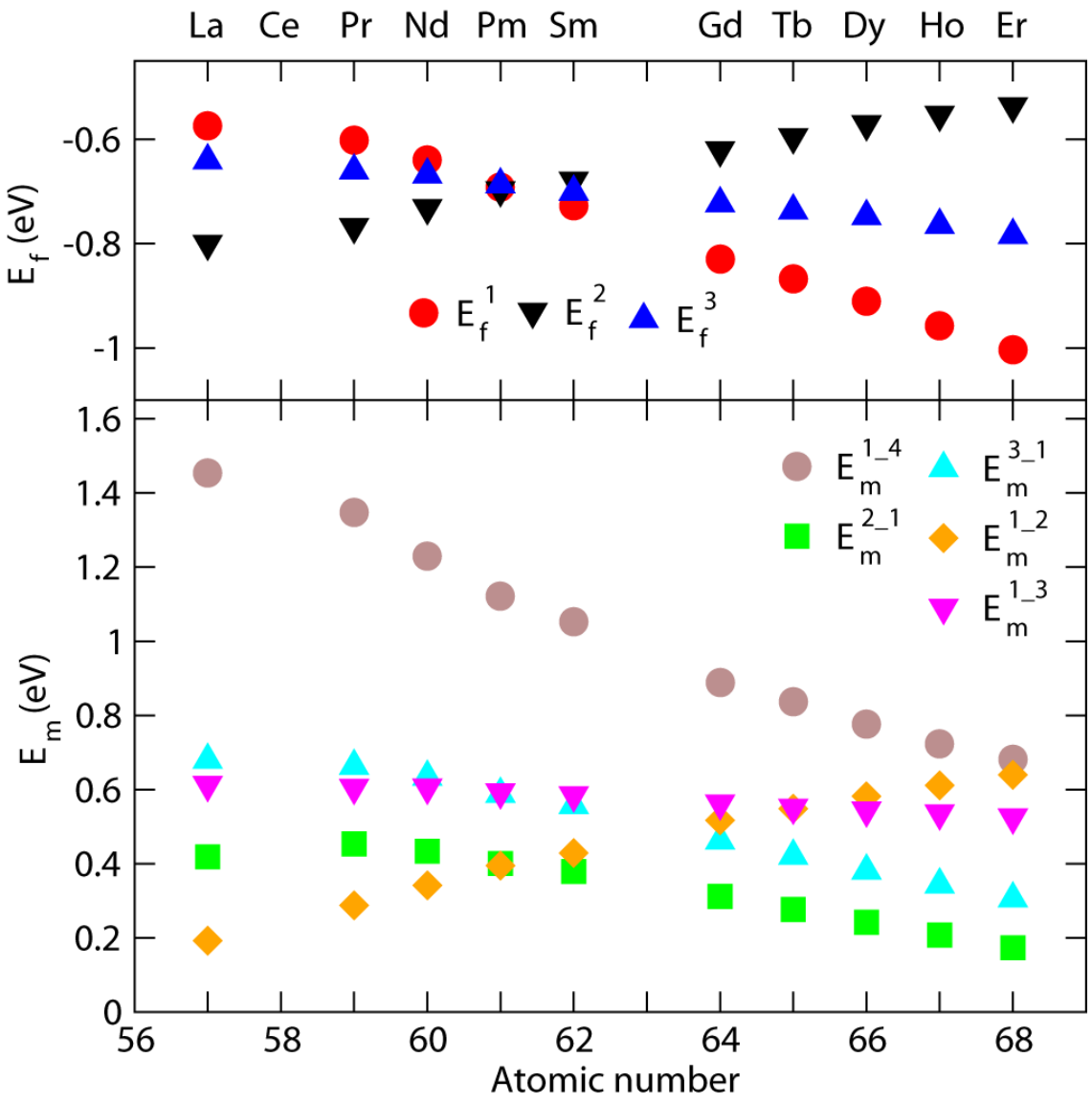

Defect formation energies

Migration barriers

(obtained for nearest neighbor 3+ dopants in the 2x2x2 supercell)

Activation Energy for Oxygen Vacancy Diffusion in Doped Ceria

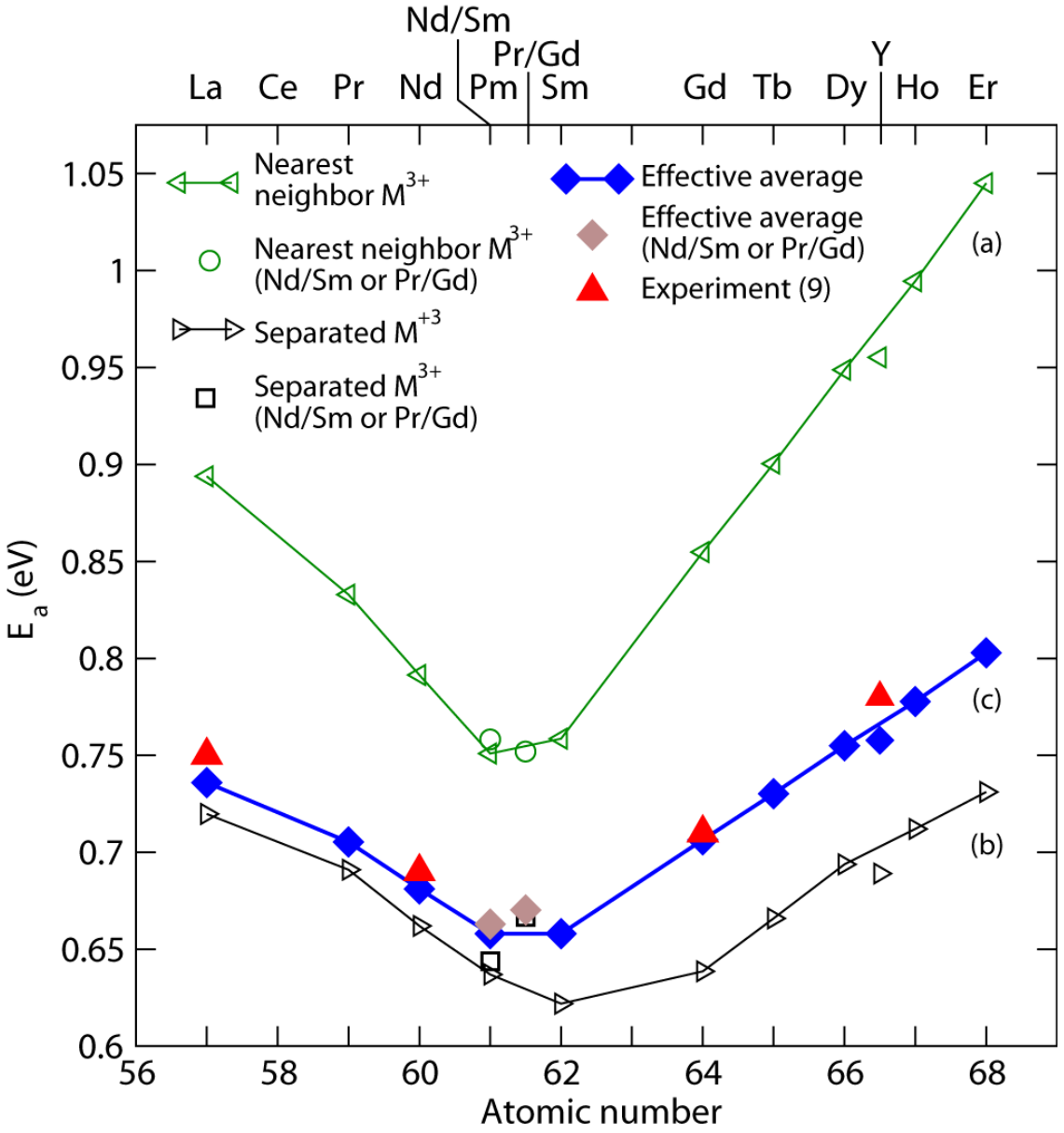

PNAS **103**, 3518 (2006)

For dopants sitting (a) next to each other, (b) separated from each other and (c) an effective average of the former two for dopant concentration 4.2%. The experimental values refer to the same doping level. Nd/Sm and Pr/Gd represent a mixture of 3+ dopants and has been placed according their average atomic numbers.


Materials design of solid electrolytes

A search of optimal materials can be done systematically instead of by trial and error.

COMMENTARY

Grain Ionic Conductivity

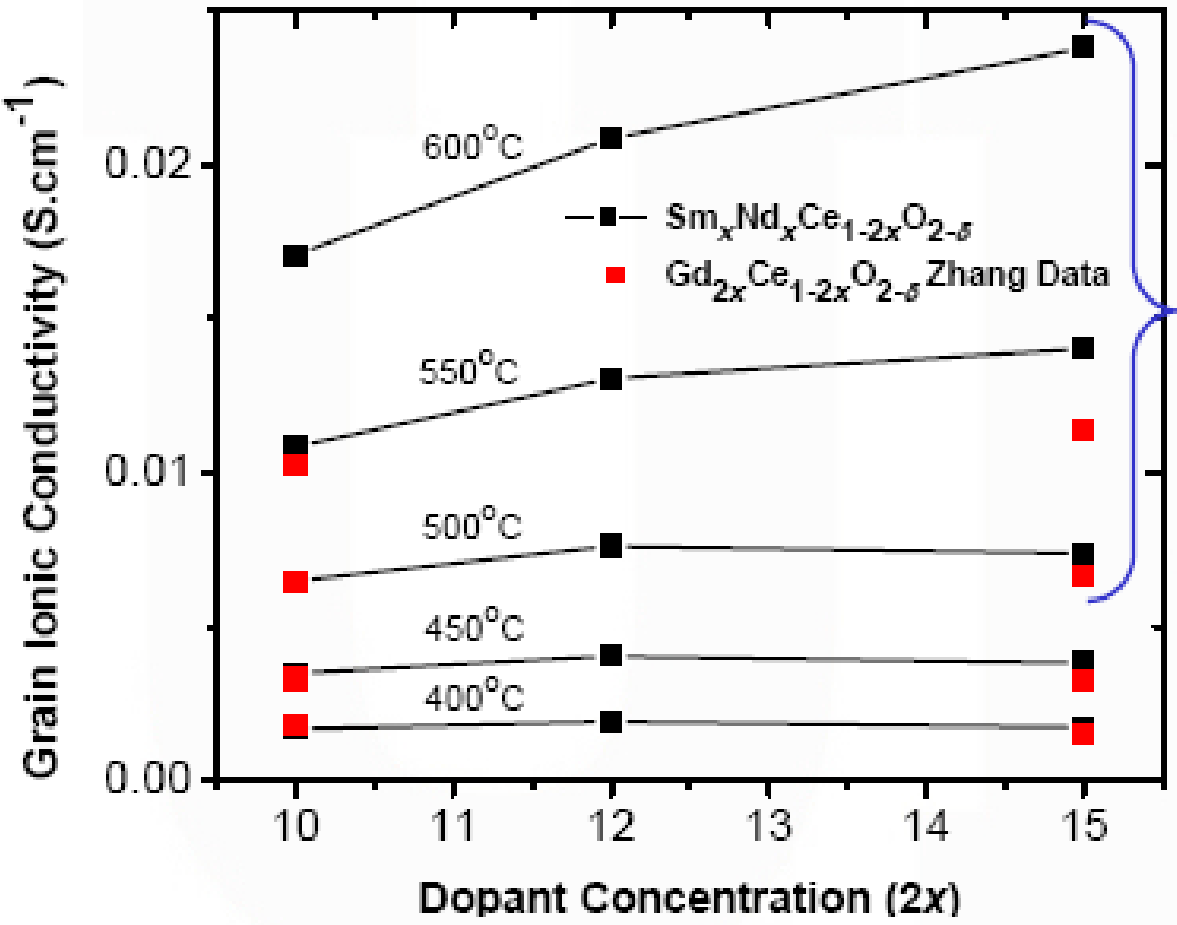

Above 500°C, the grain ionic conductivity of $Sm_{0.075}Nd_{0.075}Ce_{0.85}O_{2-\delta}$ is higher than that of $Gd_{0.10}Ce_{0.90}O_{2-\delta}$.

T. S. Zhang, J. Ma, L.B. Kong, S. H. Chan, J. A. Kilner, Solid State Ionics **170** 209-217 (2004).

Conclusions

- Our first-principles calculations of simple and complex materials are made possible thanks to modern theoretical methods and supercomputer facilities. Special thanks to NSC for excellent and constant support!
- Many more problems are going to be solved in the future:
  - Increasing number of atoms (>200) =>
  - Increasing memory requirements (> 64 Gb/32 proc)
  - Increasing CPU time (~100000 CPU hours per MD setup)
  - Scaling, optimization etc.